Geofísica Internacional (2019) 58-2: 169-178

Original paper

Coseismic displacements and Mw estimation of the El Mayor-Cucapah earthquake, Mexico, from GPS source spectra

J. Carlos Robles-Avalos, J. Alejandro González-Ortega*, J. Javier González-García and J. Antonio Vidal-Villegas

Received: August 10, 2018; accepted: November 20, 2018; published on line: April 01, 2019
DOI: http://dx.doi.org/10.22201/igeof.00167169p.2018.58.2.1968

Resumen

El sismo de magnitud Mw 7.2 El Mayor-Cucapah ocurrió el 4 de abril de 2010 en el Valle de Mexicali, cerca de la frontera entre California USA y Baja California, México. El objetivo del presente trabajo fué examinar el GPS como una herramienta complementaria en estudios sísmicos y estimar el momento sísmico del sismo y su magnitud Mw. Para ello se exploró la capacidad de los datos de GPS de alta frecuencia (5Hz) localizados en el norte de la ruptura sísmica para obtener la cinemática de los desplazamientos cosísmicos. Los datos GPS se procesaron utilizando el método de Posicionamiento Puntual Preciso con el software GIPSY-OASIS II, posteriormente se aplicó la Transformada Rápida de Fourier a las series de tiempo de posición, se calcularon los parámetros espectrales, momento sísmico y Mw. Se encontró una buena concordancia en términos de correlación de la señal de los desplazamientos GPS comparando los registros sísmicos de movimientos fuertes integrados al desplazamiento, utilizando parámetros de filtrado para dos conjuntos de instrumentos. Los espectros de desplazamiento cinemático GPS muestran un nivel de desplazamiento espectral de baja frecuencia (~0.2 Hz) cuando se compara con la doble integración de los datos de movimientos fuertes. Es fácil calcular el movimiento cosísmico estático a partir de los datos GPS. Sin embargo es muy difícil calcularlos a partir de los datos de movimientos fuertes. Un modelo simple de fuente sísmica es adecuado para el conjunto de datos GPS utilizados en este trabajo, se estimó Mw=7.19±0.13, que concuerda con el Mw 7.2 obtenido en otros estudios del sismo de El Mayor-Cucapah.

Palabras clave: Cinemática de desplazamiento cosísmico, Sismología GPS, Posicionamiento Puntual Preciso, Análisis Espectral, sismo El Mayor-Cucapah, Sismogeodesia.

Abstract

El Mayor-Cucapah earthquake Mw 7.2 on April 4, 2010, occurred on Mexicali Valley near the international border between California, USA and Baja California, Mexico. The objective of this paper was to examine GPS as a complementary tool for seismic studies and to estimate earthquake seismic moment and Mw. For this purpose the capabilities of high-rate GPS (5 Hz) data located in the northern part of the seismic rupture has been explored to obtain the kinematic coseismic displacements. GPS data were processed using Precise Point Positioning method with GIPSY-OASIS II software, then applying the Fast Fourier Transform to the position time series, spectral parameters, seismic moment and Mw were calculated. A good agreement was found in terms of signal correlation of the GPS displacements, by comparing strong-motion seismic records integrated to displacement, using filtering parameters for two sets of instruments. Kinematic GPS displacement spectra clearly shows the low frequency displacement spectral level (~0.2 Hz) when compared with double integration of strong-motion data. It is easy to calculate the static coseismic motion from GPS data, however it is very difficult to calculate it from strong-motion data. A simple earthquake source model is suitable for the GPS dataset used in this work, estimated on Mw=7.19±0.13, was in according with Mw 7.2 obtained in other studies of the El Mayor-Cucapah earthquake.

Key words: Kinematic coseismic displacement, GPS Seismology, Precise Point Positioning, Spectral Analysis, El Mayor-Cucapah earthquake, Seismogeodesy.

J. C. Robles-Avalos
Posgrado en la División de Ciencias de la Tierra
Centro de Investigación Científica
y de Educación Superior de Ensenada
Baja California, Ensenada
B.C. México

J. A. González-Ortega*
J. J. González-García
J. A. Vidal-Villegas
Departamento de Sismología
División de Ciencias de la Tierra
Centro de Investigación Científica
y de Educación Superior de Ensenada
Baja California, Ensenada
B.C. México
*Corresponding author: aglez@cicese.mx

Introduction

El Mayor-Cucapah earthquake has provided an important opportunity to study about the geodynamics of the northwest region of Mexico (Fletcher *et al*., 2016), as spatial and tectonic geodesy (Wei *et al*., 2011). The use of GPS in seismology was first documented by Hirahara *et al*., (1994), Ge *et al*., (2000) and Nikolaidis *et al*., (2001), who demonstrate the potential of GPS as a seismological instrument. For instance, Larson *et al*., (2003) using GPS (1 Hz) achieved to observe the kinematic displacements of the Alaska Denali earthquake (*Mw* 7.9) in 2002, suggesting that GPS observations are crucial to study rupture processes. Miyazaki *et al*., (2004) compared displacements from GPS with the double integration of the acceleration records, finding a good correlation between both for the Tokachi-Oki earthquake (*Mw* 8.3, occurred in 2003). Blewitt *et al*., (2006) demonstrated the GPS ability to estimate the magnitude of a megathrust earthquake, using data from up to only a few minutes after earthquake initiation, as well as its high tsunamigenic potential for the Sumatra–Andaman earthquake (*Mw* 9.2-9.3) in 2004; whereas, Hung *et al*., (2017) shown that 5 Hz high-rate GPS observations is an optimal sampling rate for GPS seismology as observed for the Ruisi Taiwan earthquake occurred in 2013. Nowadays, broadband and/or strong-motion seismic instruments located with high-rate GPS receivers are the best instrumental candidates to measure the complexity in the seismic source, rapid slip characterization of finite fault rupture and also for applications on early seismic warning systems (Melgar *et al*., 2013; Bock *et al*., 2011; Bock and Melgar, 2016).

Northern Baja California tectonics is primary dominated by right-lateral strike slip of ~50 mm/yr along southernmost San Andreas Fault system, between the Pacific and North American plates (Argus *et al*., 2010; DeMets *et al*., 2010) (Figure 1-inset). The El Mayor-Cucapah earthquake (32.278° N, 115.339° W; 4 km Depth; Mw 7.1; To=2010-04-04 22:40:40 UTC; RESNOM Database) of April 4, 2010, Mw 7.2, had a complex bidirectional rupture divided into two main domains from the epicentral zone located in the southeast corner of the Sierra Cucapah mountain range (Hauksson *et al*., 2010; Fletcher *et al*., 2014). The rupture in the northern section spread through the Cucapah mountains by several multiple faults-segments: Pescadores, Borrego, Paso Superior e Inferior. While in the southern section it extended through the Colorado River Delta, where it was possible to identify a new fault named Indiviso. The extent of the rupture was around 120 km (Figure 1) (González-García *et al*., 2010; Wei *et al*., 2011, Fletcher *et al*., 2014).

The characterization of a seismic source depends primarily on the direction of propagation of the seismic waves, distribution of the rupture and the magnitude of the coseismic displacements (Hanks, 1981). One way to estimate earthquake source parameters (seismic moment, stress drop and source radius) is computing the Fast Fourier Transform (FFT) to the displacements in the far-field (Savage, 1972), and getting the spectral parameters (level at low frequencies, corner frequency and slope to high frequencies), to obtain the seismic moment (M_0) (Brune, 1970), and then the moment magnitude (Mw) (Hanks and Kanamori, 1979) of an earthquake.

High-rate GPS (from 1-10 Hz) displacements has been proved very useful for monitoring long-period ground motion, moreover, the optimal combination of near-source GPS and seismic strong-motion data covers a broad spectrum of coseismic motion, from high frequencies to long periods (Bock and Melgar, 2016). Taking advantage of the availability of high-rate GPS records (5 Hz) nearby the seismic rupture of the El Mayor-Cucapah earthquake, the position ground motion was obtained, and then the results were compared with the double integration of acceleration data, for two sets of located (close to each other) GPS and strong-motion instruments. In the case of acceleration data a first order Butterworth filter was used within 0.10 – 50 Hz (Bendat and Piersol, 2011; Oppenheim and Shafer, 2011) in the frequency domain, while not for the GPS position. Finally, the earthquake seismic moment was estimated using a simple earthquake source model (Brune, 1970; Kumar *et al*., 2012) and moment magnitude was obtained following Hanks and Kanamori (1979).

Data and Methods

High-rate GPS (5Hz) data were used from the Plate Boundary Observatory GPS network (Figure 1), obtained through the University NAVSTAR Consortium (UNAVCO) and acceleration data from Southern California Earthquake Data Center (SCEDC), and Center for Engineering Strong Motion Data (CESMD) for the El Mayor-Cucapah earthquake.

The technique used to process the GPS data was Precise Point Positioning (PPP) with GIPSY-OASIS software (Zumberge *et al*., 1997; Kouba and Heroux 2001). PPP is a positioning technique that is based on precise

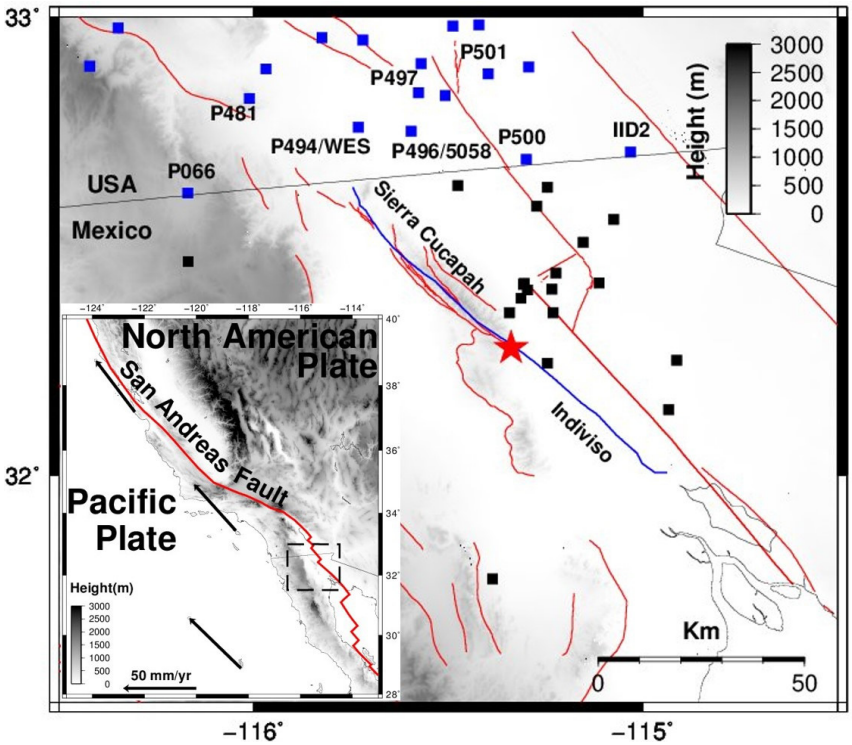

Figure 1. Tectonic setting of the north Baja California region, where the El Mayor-Cucapah earthquake occurred. The red star denotes the earthquake epicenter. Blue line denotes the surface rupture [Fialko *et al.,* 2010] and red lines denote known active faults. Blue squares denote GPS continuous recording sites in USA during the earthquake occurrence and black squares are GPS temporal surveyed sites after the earthquake (González-Ortega *et al*., 2014). P494/WES and P496/5058 are colocated GPS and strong-motion instruments; as well as, P066, P481 P497, P50, P500 and IID2 are GPS stations used in the present study. Inset illustrates a broader tectonic setting of the study area. Black vectors shows the tectonic motion with respect to North American Plate.

position coordinates obtention for a single station without a reference station, using precise orbit products and clock corrections provided by the International GNSS Service (IGS) (Abdallah and Schwieger, 2014). This technique can be used for both kinematic and static GPS processing. To achieve centimeter-level accuracy estimates, several modeling effects must be taken into account, such as the atmospheric effects on the carrier phase, as well as terrestrial and oceanic tides (Heroux *et al*., 2001). Thus, from far-field displacements in the frequency domain, earthquake seismic moment and magnitude can be obtained (Hanks and Wyss, 1972; Johnson and McEvilly, 1974).

The simplest and widely used earthquake source models are those proposed by: Haskell (1964) and Brune (1970). In the Haskell's model, two corner frequencies $f_r = \frac{2}{t_r}$ and $f_d = \frac{2}{t_d}$ are defined. Where t_r is rupture time and t_d is rise time. The spectrum is flat for frequencies less than f_r, then goes as f^{-1} between f_r and f_d, to finally decay as f^{-2} for high frequencies. Thus the spectrum is parametrized by three factors, seismic moment Mo, raise time t_d and rupture time t_r (Stein and Wysession, 2003). The Brune's model has a single corner frequency, f_c, that combines the effects of rise and rupture time. The amplitude spectrum corresponds to displacements observed in the far-field; however, it is also applicable for observations in the near-field as long as the source-receiver distance is greater than the wavelength of the seismic waves (Madariaga, 1989). In the present case, a wavelength of ~26 km is obtained when considering seismic wave velocity of 3.3 km/s (Fuis *et al*., 1982) and 8 s period of the first oscillation for P494 station (Figure 2).

One of the most important spectral parameter is the flat line-segment of the amplitude spectrum at low frequencies as proposed by Haskell (1964) and Brune (1970). This frequency line-segment is commonly referred as Ω_0, spectral level to low frequencies, from this parameter seismic moment is (Brune, 1970; Archuleta *et al*., 1982),

$$M_o = \frac{\Omega_0}{F_s R_{\theta\phi}} 4\pi\rho R\beta^3 \quad (1)$$

Where Ω_0 is the line-segment at low frequencies, $R_{\theta\phi}$ is the average radiation pattern for *S* waves (~0.6), ρ is the density of the medium (2.75 $\frac{g}{cm^3}$) and β the s-wave velocity (3.3 x 10^5 $\frac{cm}{s}$) (Fuis *et al*., 1982), R is the distance from the hypocenter to the observation site and Fs is the free surface factor (2). Finally, we used the moment magnitude relation proposed by Hanks and Kanamori [1979], in which *Mo* is in units of dyne-cm,

$$Mw = \frac{2}{3} logM_o - 10.7 \quad (2)$$

Results

GPS position time series corresponding to the nearest sites to the earthquake rupture are shown in Figure 2. The kinematic displacement generated by the passage of the seismic waves can be observed, as well as the coseismic permanent displacement, derived from the surface motion of the El Mayor-Cucapah earthquake. Differences in amplitude and oscillation are due to the type of soil and epicentral distance. P494 is located ~65 km from the epicenter in the west Salton Sea basin; while P481 is ~87 km in the Peninsular Ranges. To estimate the coseismic displacements, the linear trend of the surperficial pre-arrival seismic wave was first calculated and then the entire record of the

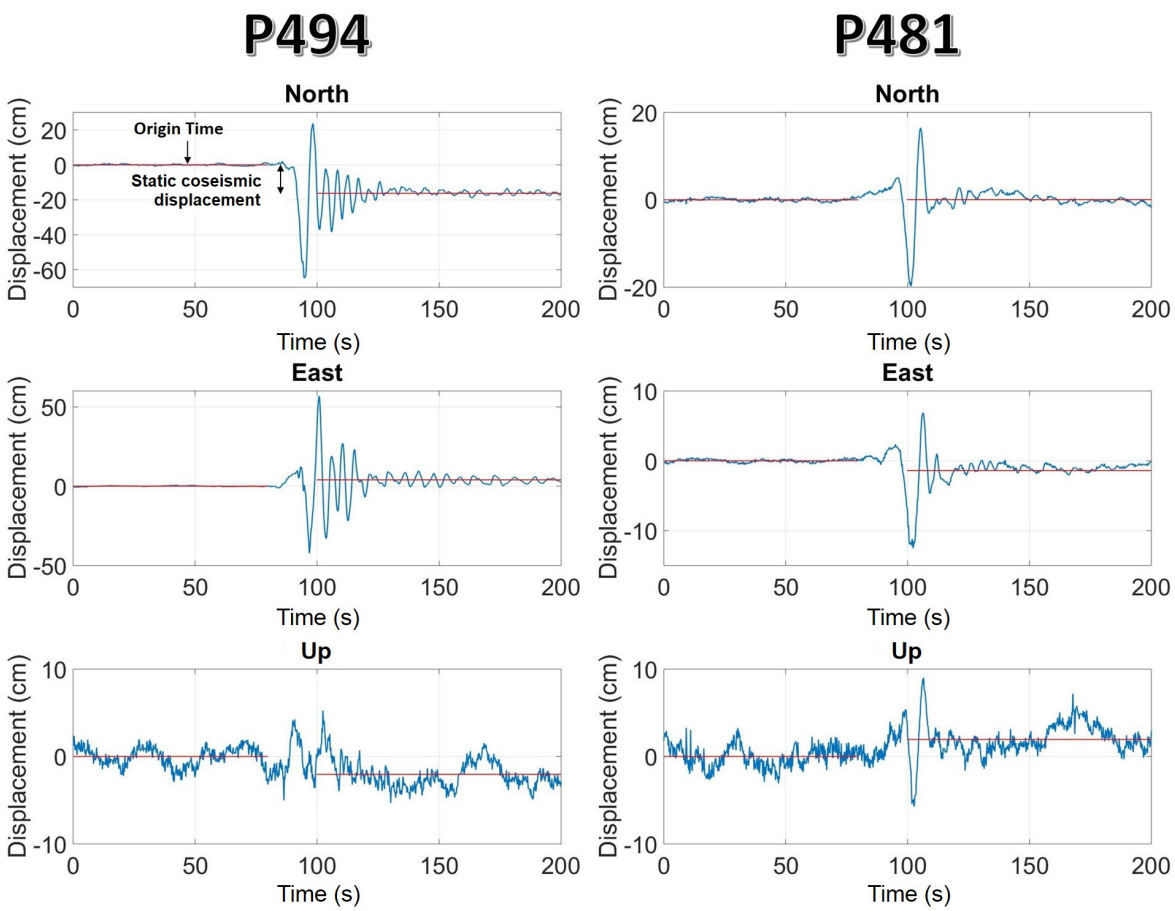

Figure 2. GPS position time series. Left column, GPS site P494, ~65 km from epicenter. Right column, GPS site P481, ~87 km from epicenter. Red lines indicate linear detrend removed before and after the S-wave arrival to estimate the static coseismic offsets.

position time series. Subsequently, the mean of the oscillations of the pre-arrival and post-arrival segments was calculated, the difference between both segments corresponds to the static (permanent) coseismic displacement. In Table 1, the kinematic and static coseismic displacements for GPS sites processed in this study are presented.

GPS position time series were compared with the displacement series obtained from the double integration of the accelerometer records from WES and 5058 accelerograph stations, located at <1 km from GPS sites P494 and P496, respectively (Figure 3). Horizontal components show alignment in phase and similarity in amplitudes (see inset plots). For strong-motion data several tests to find the frequency range and order for the Butterworth filter were performed. First-order Butterworth bandpass filter was selected, from 0.08 and 0.20 to Nyquist frequency for WES and 5058 respectively. This type of filter allows to improve the position of the time series and to carry out the comparison with GPS position time series. High order Butterworth filters tend to generate biases in position baseline and cause distortions [Oppenheim and Schafer, 2011].

To compare the kinematic GPS displacements and double integrated accelerogram data, a normalized cross-correlation was used. In general, correlation values are better in the east-west (>0.90) than north-south (>0.70), due to the smaller kinematic coseismic displacement in the east-west direction. Consequences of seismic filtering tends to diminish the amplitudes of the displacement series obtained from

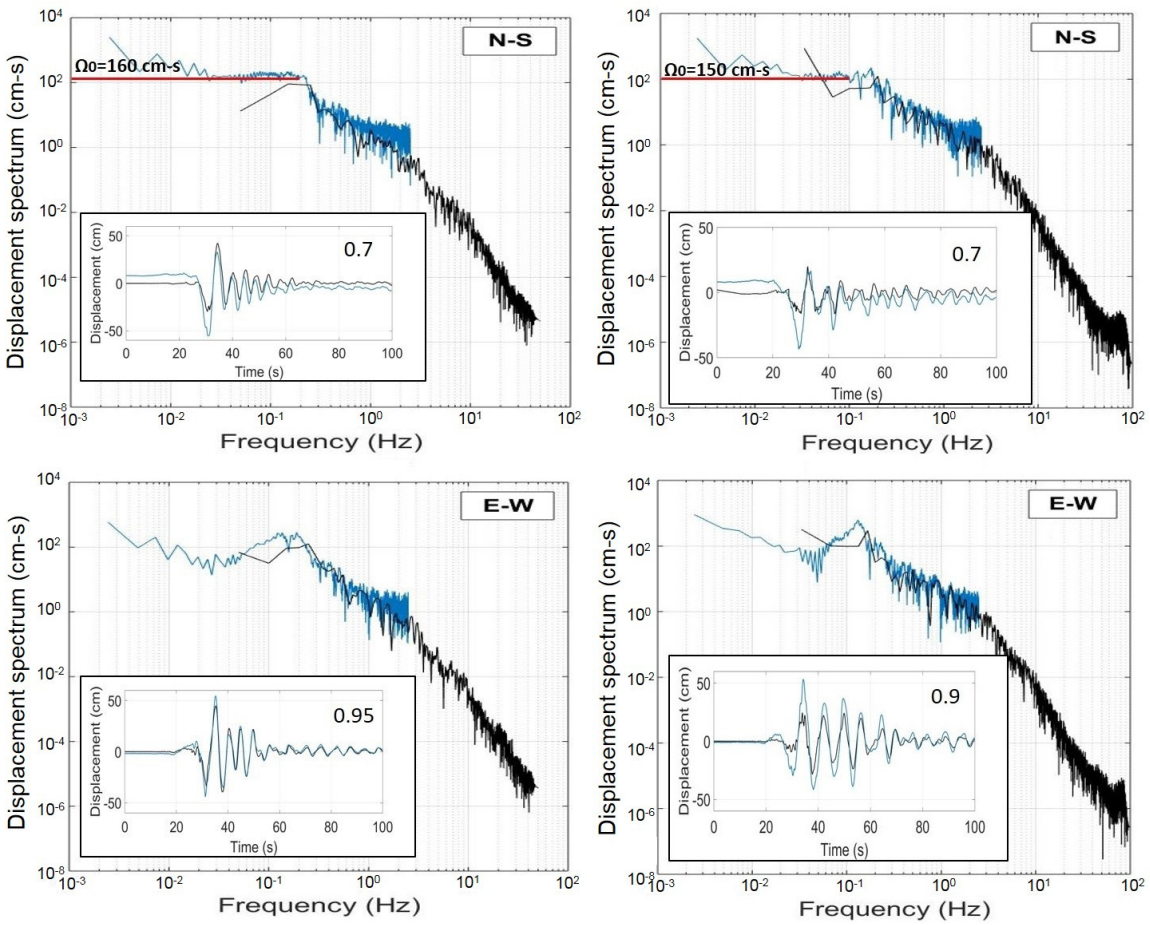

Figure 3. Displacement spectrum comparisons from collocated strong motion (black) and high-rate GPS (blue). Left column, horizontal displacement spectrum at P494-GPS and WES accelerograph station. Right column, horizontal displacement spectrum at P496-GPS and 5058 accelerograph station. Red horizontal lines indicate Ω_0 value. Insets show comparison between GPS and integrated (from strong-motion) time series displacement and corresponding cross-correlation values estimate.

Table 1. 3D Coseismic displacements estimates from GPS position time series. Includes earthquake distance to GPS sites, peak-to-peak oscillation seismic wave motion, flat line segment amplitude value at low frequencies Ω_o, M_o and M_w.

GPS site	Lat.	Long.	Epicentral distance (km)	Kinematic peak to peak oscillation, north (cm)	Kinematic peak to peak oscillation, east (cm)	Kinematic peak to peak oscillation, Up (cm)	Static coseismic north (cm)	Static coseismic east (cm)	Static coseismic Up (cm)	Ω_o (cm-s)	M_o (dyne-cm) 1x10^{26}	M_w
P494	32.760	-115.732	65	90	100	10	-18	4	~ -1	160	10.8	7.32
P496	32.751	-115.596	58	60	95	24	-17	~2	~0	150	9.0	7.27
P497	32.835	-115.577	67	40	60	15	-9	~1	~1	125	8.7	7.26
P501	32.876	-115.398	67	45	36	10	-5	~2	~1	137	9.5	7.29
P500	32.690	-115.300	46	26	30	12	-4	5	~0	93	4.4	7.06
IID2	32.706	-115.032	54	16	21	NA	~ -2	3	~0	77	4.3	7.06
P481	32.822	-116.012	87	36	20	15	~ -2	~ -1	~0	74	6.7	7.18
P066	32.617	-116.170	90	16	11	13	~0	-7	~0	51	4.8	7.08

accelerogram double integration data when compared to those obtained with GPS. Static coseismic displacements are not observable in strong-motion due to wideband limitation but in GPS these are clearly captured.

Figure 3 shows horizontal GPS and strong-motion source spectra comparison for P494-GPS and WES, as well as, P496-GPS and 5058. With GPS spectra, the amplitude at low frequencies Ω_0 is easily identified. After a value of ~0.2Hz, amplitudes decay at f^{-2} as frequency increases up to where GPS spectra turns constant. At this point, seismic oscillations with spectral amplitudes of ~2cm·s associated with frequency values ~1Hz (periods ≥ 1 s for 5Hz GPS sampling rate), are not detectable with GPS. On the other hand, with strong-motion displacement spectra, two corner frequencies at ~0.2Hz and ~3Hz can be identified. For frequencies >3Hz amplitude decay as f^{-4}. These amplitude decays are related to attenuation and site effects [Shearer, 1999].

Seismic moment (M_o) and moment magnitude (M_w) of the El Mayor-Cucapah earthquake is M_o = 7.3±3.5x10^{26} dyne-cm, M_w = 7.19±0.13 using GPS spectra (Table 1), and *Mo* = 6.4±0.07x10^{26} dyne-cm, M_w = 7.14±0.01, using WES and 5058 strong-motion data spectra. These values are similar to estimates obtained from seismic and geodetic data inversion M_o = 9.9x10^{26} dyne-cm, M_w = 7.26 [Wei *et al*., 2011] and from field measurements of M_o = 7.2x10^{26} dyne-cm, M_w = 7.17 [Fletcher *et al*., 2014].

Figure 4 shows the El Mayor-Cucapah static coseismic horizontal displacements. The maximum horizontal static coseismic displacement is ~1.16 m, in the N137°E direction, ~8 km from the epicenter, in the southeastern part of the Sierra Cucapah, and the maximum vertical displacement is ~-0.64 m. The displacement pattern, clearly observed in the northeast is consistent with a right-lateral focal mechanism of The El Mayor-Cucapah earthquake (González-Ortega *et al*., 2014). These authors, estimated earthquake moment magnitude using dislocation inversion methods from a finite coseismic slip model composed of several fault segments using GPS and InSAR static displacements in a homogeneous (Fialko *et al.,* 2010) and in an layered earth structure [Huang *et al*., 2016].

Discussion

Zheng *et al*., (2012), also used high-rate GPS data with the aim of carrying out the seismotectonics analysis of El Mayor-Cucapah earthquake with different methodology as in this work. They used the Cut and Paste method (CAP) developed by Zhu and Helmberger (1996), which allows separating the P_n and surface waves independently, not requiring an accurate crustal velocity model or a high number of stations, but a good azimuthal coverage for the focal mechanism inversion and earthquake magnitude. Also, Allen and Ziv (2011), re-processed in a simulated real-time high-rate GPS static displacement data, to estimate earthquake magnitude via static slip inversion, using preliminary earthquake hypocenter from seismic data and a catalog of active faults, for the purpose of earthquake early warning system test in southern California.

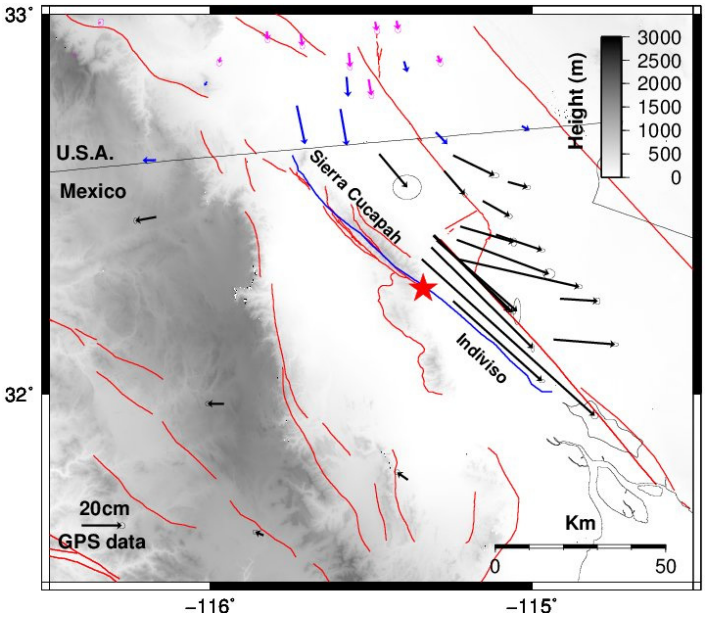

Figure 4. GPS horizontal coseismic displacements from El Mayor-Cucapah earthquake. Blue vectors are estimates obtained in this study. Black are displacements from Gonzalez-Ortega (2014), and magenta are from GPS Explorer Data Products (http://geodemo-c.ucsd.edu). The red star denotes the earthquake epicenter. Blue line denotes the surface rupture [Fialko *et al.,* 2010] and red lines denote known active faults.

Differences between Zheng *et al*., (2012), and the present work lies in the GPS data processing; while we used the PPP technique, they used the Double Differences (DD). For the DD technique (Herring *et al.*, 2015) it is necessary to have a reference station, which must be located at a distance far enough to not be affected by seismic waves, but close enough to act as reference station which guarantees the same satellites observation of the sites of interest. Such condition is not required with PPP technique, as it uses precise GPS orbit and clock data products with centimeter accuracy. Although the methodology used in Zheng *et al*., (2012) and the present one differ in estimating GPS time series and seismic moment, in general, position time series and moment magnitude results are very similar and confirm earlier studies using GPS high-rate data from El Mayor-Cucapah earthquake (Allen and Ziv, 2011; Bock *et al.*, 2011).

With high-rate GPS spectral analysis, amplitude at low frequencies is clear to identify in contrast to accelerogram data. This flat low frequency section is associated with large displacement amplitudes generated by the passage of surperficial seismic waves (Udias, 1989). Thus, estimates of M_o and M_w can have a greater degree of certainty with GPS data than with accelerometer records. GPS data can be of crucial importance for estimating major earthquake magnitude in real time (Blewitt *et al.*, 2006; Bock and Melgar, 2016). According to the present results, average Ω_0 value with GPS data is 115±4 cm-s, while with accelerogram data is 90±8 cm-s. However, as GPS is sampled at 5 Hz, for frequencies >2.5 Hz (Nyquist frequency) GPS is unable to observe spectral displacements below 2 cm-s, which does not happen with the acceleration records. This highlights the importance of the complementarity between both instruments, closely located GPS and strong-motion, for near field displacements earthquake studies.

Conclusion

High-rate (5 Hz) kinematic GPS position time series of the El Mayor-Cucapah earthquake were studied and compared to the displacement series obtained from the double integration of strong-motion data. The comparison shows good agreement in terms of cross-correlation, for P494-GPS and WES, and, P496-GPS and 5058, instruments at ~75 km from epicenter. Kinematic GPS data at low frequencies, associated with large spectrum displacements, help to clearly identify the flat line segment amplitude better than accelerogram data, and thus using a simple earthquake source model the earthquake seismic moment, Mo=7.3±3.5x10^{26} dyne-cm, Mw=7.19±0.13 could be estimated, similar

to Mw 7.2 as previously reported using other methodologies. Static coseismic displacements are very difficult to obtain from accelerogram data, however with GPS data, these are easily obtained and consistent with the right-lateral strike-slip mechanism of the El Mayor-Cucapah earthquake.

Data and Resources

High-rate GPS data can be found at UNAVCO, ftp://data-out.unavco.org/pub/highrate/5-Hz/rinex/ (last accessed April 2018). Coseismic displacements from the northern side of the El Mayor-Cucapah rupture can be found at GPS Explorer, http://geodemo-c.ucsd.edu (last accessed April 2018). Accelerometric data can be found at SCEDC, http://scedc.caltech.edu/research-tools/waveform.html (last accessed April 2018) and CESMD, https://www.strongmotioncenter.org/cgi-bin/CESMD/search_options.pl (last accessed April 2018). Map figures were generated by Generic Mapping Tool (GMT) software [Wessel *et al*., 2013].

Acknowledgments

The authors would like to thank Editor Dr. Manuel Berrocoso-Dominguez and two anonymous reviewers for their valuable suggestions. This work was partially financially supported by CONACyT though a graduate scholarship to Robles-Avalos J.C. (2015-2017). We thank Dr. Sara Ivonne Franco Sánchez and Dr. Luis Mungía Orozco for their comments during this work. Also we acknowledge to local people during the GPS campaigns in northern Baja California.

References

Abdallah, A. and Schwieger, V. (2014). Accuracy Assessment Study of GNSS Precise Point Positioning for Kinematic Positioning. In Schattenberg, J., Minßen, T. F.: Proceeding on 4th International Conference on Machine Control and Guidance (MCG), Braunschweig: Institut für mobile Maschinen und Nutzfahrzeuge, Braunschweig, Germany.

Allen, R. M. and Ziv, A. (2011). Application of Real-Time GPS to earthquake early warning. Geophysical Research Letters, 38, L16310.

Archuleta, R. J., Cranswick, E., Mueller, C., and Spudich, P. (1982). Source parameters of the 1980 Mammoth Lakes, California, earthquake sequence. Journal of Geophysical Research: Solid Earth, 87(B6), 4595-4607.

Argus, D.F., Gordon, R.G., Heflin, M.B., Ma, Ch., Eanes, R.J., Willis, P., Peltier, W.R. and Owen, S.E. (2010). The angular velocities of the plates and the velocity of Earth's center from space geodesy. Geophysical Journal International, 180(3), 913-960.

Bendat, J.S., Piersol, A.G. (2011). Random Data: Analysis and Measurement Procedures. John Wiley & Sons. 640 pp.

Blewitt, G., Kreemer, C., Hammond, W. C., Plag, H. P., Stein, S., and Okal, E. (2006). Rapid determination of earthquake magnitude using GPS for tsunami warning systems. Geophysical Research Letters, 33(11).

Bock, Y. and Melgar D. (2016). Physical applications of GPS geodesy: a review. Reports on Progress in Physics. 79, 106801, 119 p.

Bock, Y., Melgar, D., and Crowell B.W. (2011). Real-time strong motion broadband displacement from collocated GPS and accelerometers. Bulletin of the Seismological Society of America. 101(6). 2904-2925.

Brune, J. N. (1970). Tectonic stress and the spectra of seismic shear waves from earthquakes. Journal of Geophysical Research, 75(26), 4997-5009.

DeMets, C., Gordon, R.G. and Argus, D.F. (2010). Geologically current plate motions. Geophysical Journal International, 181(1), 1-80.

Fialko, Y., A. González, J. González, S. Barbot, S. Leprince, D. Sandwell, and D. Agnew (2010), Static rupture model of the 2010 Mw 7.2 El Mayor-Cucapah earthquake from ALOS, ENVISAT, SPOT and GPS data, Abstract T53B-2125 presented at 2010 Fall Meeting, AGU, San Francisco, Calif.

Fletcher, J., Teran, O.J., Rockwell, T. K., Oskin, M., Hudnut, K. W., Mueller, K. J. Spelz, R. M., Akciz, S. O., Masana, E., Faneros, G., Fielding, E. J., Leprince, S., Morelan, A. E., Stock, J. Lynch, D. K. Elliott, A. J., Gold, P., Liu-Zeng, J., González-Ortega, A. Hinojosa-Corona, A., and González-García, J. (2014). Assembly of a large earthquake from a complex fault system: Surface rupture kinematics of the 4 April 2010 El Mayor–Cucapah (Mexico) Mw 7.2 earthquake. Geosphere, 10 (4), 797-827.

Fletcher, J.M., M.E. Oskin, and Teran, O.J. (2016). The role of a keystone fault in triggering the complex El Mayor–Cucapah

earthquake rupture. Nature Geoscience, 9, 303–307.

Fuis, G.S., Mooney, W.D., Healey, J.H., McMechan G.A., and Lutter, W.J. (1982). Crustal structure of the Imperial Valley region. USGS professional paper 1254, 25-50.

Ge, L., Han, S., Rizos, C., Ishikawa, Y., Hoshiba, M., Yoshida, Y. and Himori, S. (2000). GPS seismometers with up to 20 Hz sampling rate. Earth, planets and space, 52(10), 881-884.

González-García, J. J., J. A. González Ortega, Y. Bock, Y. Fialko, E. J. Fielding, J. Fletcher, J. E. Galetzka, K. W. Hudnut, L. Munguia, and S. M. Nelson. (2010). Seismotectonics of the 2010 El Mayor Cucapah—Indiviso earthquake and its relation to seismic hazard in southern California, Abstract T53B-2117 presented at 2010 Fall Meeting, AGU, San Francisco, Calif.

González-Ortega, A., Y. Fialko, D. Sandwell, F. Alejandro Nava-Pichardo, J. Fletcher, J. González-García, B. Lipovsky, M. Floyd, and G. Funning (2014), EL Mayor-Cucapah (Mw7.2) earthquake: Early near-field posteismic deformation from InSAR and GPSobservations, J. Geophys. Res. Solid Earth, 119, 1482-1472.

González-Ortega, J. A., (2014). Análisis sismo-geodésico del sismo El Mayor-Cucapah (Mw=7.2) del 4 de abril de 2010, Baja California Tesis de doctorado en ciencias. Centro de Investigación Científica y de Educación Superior de Ensenada, Baja California.

Hanks, T. (1981). The Corner Frequency Shift, Earthquake Source Models, and Q. Bulletin of the Seismological Society of America. 71 (3); pp. 597-612.

Hanks, T. and Kanamori, H. (1979). A moment magnitude scale. Journal of Geophysical Research. 84(B5), 2348–2350.

Hanks, T. and Wyss, M. (1972). The use of body-wave spectra in the determination of seismic-source parameters. Bulletin of the Seismological Society of America, 62(2), 561-589.

Haskell, N. (1964). Total energy and energy spectral density of elastic wave radiation from propagating faults. Bulletin of the Seismological Society of America, 54, 1811-1841.

Hauksson, E., Stock, J., Hutton, K., Yang, W., Vidal-Villegas, J.A. and Kanamori, H. (2010). The 2010 Mw 7.2 El Mayor-Cucapah Earthquake Sequence, Baja California, Mexico and Southernmost California, USA: Active Seismotectonics along the Mexican Pacific Margin. Pure Applied Geophysics. 168, 1255–1277.

Heroux, P., Kouba, J., Collins, P., and Lahaye, F. (2001). GPS carrier phase point positioning with precise orbit products. In Procedings of the KIS, 5-8. Pierre Heroux Geodetic Survey Division, Natural Resources Canada.

Herring, T. A., R. W. King, M. A. Floyd, and S. C. McClusky (2015). Introduction to GAMIT/GLOBK, Release 10.6, Mass. Inst. Of Technol., Cambridge, Massachusetts.

Hirahara, K., Nakano, T. and Hoso, Y. (1994). An experiment for GPS strain seismometer. In Proceeding of Japanese Symposium on GPS. pp. 67-75. 15-16 December, Tokio, Japan.

Huang, M.-H., E. J. Fielding, H. Dickinson, J. Sun, J. Alejandro González-Ortega, A. M. Freed, and R. Bürgmann (2016). Fault Geometry Inversion and Slip Distribution of the 2010 Mw 7.2 El Mayor-Cucapah Earthquake from Geodetic Data, J. Geophys. Res. Solid Earth, 121, 607-622.

Hung, H-K, Rau, R-J., Benedetti, E., Branzanti, M., Mazzoni, A., Colosimo, G., and Crespi, M. (2017). GPS Seismology for a moderate magnitude earthquake: Lessons learned from the analysis of the 31 October 2013 ML 6.4 Ruisui (Taiwan) earthquake. Annals of Geophysics, 60, 5, 2017; S0553.

Johnson, L. R., and McEvilly, T. V. (1974). Near-field observations and source parameters of central California earthquakes. Bulletin of the Seismological Society of America, 64(6), 1855-1886.

Kouba, J., and Heroux, P. (2001). Precise point positioning using IGS orbit and clock products. GPS solutions, 5(2), 12-28.

Kumar A., Kumar, A., Mittal, H., Kumar, A., and Bhardwaj, R. (2012). Software to Estimate Earthquake Spectral and Source Parameters. International Journal of Geosciences, 3, 1142-1149.

Larson, K. M., Bodin, P., and Gomberg, J. (2003). Using 1-Hz GPS data to measure deformations caused by the Denali fault earthquake. Science, 300(5624), 1421-1424.

Madariaga, R. (1989). Propagación de Ondas Sísmicas en el campo cercano. Física de la Tierra, 1, 51-73. Ed. Universidad Complutense Madrid.

Melgar, D., Crowell B.W., Bock Y. and Hasse J.S. (2013). Rapid modelling of the 2011 Mw 9.0 Tohoku-Oki earthquake with seismogeodesy. Geophysical Research Letters, 40(12).2963-2968.

Miyazaki, S. I., Larson, K. M., Choi, K., Hikima, K., Koketsu, K., Bodin, P. and Yamagiwa, A. (2004). Modeling the rupture process of the 2003 September 25 Tokachi Oki (Hokkaido) earthquake using 1 Hz GPS data. Geophysical Research Letters, 31(21).

Nikolaidis, R.M., Bock Y., de Jonge P.J., Shearer P., Agnew D.C. and Van Domselaar M. (2001). Seismic wave observations with the Global Positioning System. Journal of Geophysical Research, 106 (10) 21879-21916.

Oppenheim A., and Schafer R. (2011). Digital Signal Processing. Prentice-Hall of India Pvt. Limited. 585 pp.

Savage, J. C. (1972). Relation of corner frequency to fault dimensions. Journal of Geophysical Research, 77(20), 3788-3795.

Shearer P. (1999). Introduction to seismology. Cambridge University Press.

Stein, S., and Wysession, M. (2003). An introduction to seismology, earthquakes, and earth structure. Blackwell Pub.

Udias, A. (1989). Parámetros del foco de los terremotos. Física de la Tierra, 1, 87-104. Ed. Universidad Complutense Madrid.

Wei, S., Fielding, E., Leprince, S., Sladen, A., Avouac, J.P., Helmberger, D., Hauksson, E., Chu, R., Simons, M., Hudnut, K., Herring, T., Briggs, R. (2011). Superficial simplicity of the 2010 El Mayor–Cucapah earthquake of Baja California in Mexico. Nature Geoscience 4, 615-618.

Wessel, P., W. H. F. Smith, R. Scharroo, J. Luis, and F. Wobbe (2013), Generic mapping tools: Improved version released, EOS Trans. AGU, 94(45), 409–410.

Zheng, Y., Li, J., Xie, Z., Ritzwoller, M.H. (2012). 5 Hz GPS seismology of the El Mayor-Cucapah earthquake: estimating the earthquake focal mechanism. Geophysical Jounal International, 190, 1723-1732.

Zhu, L., and Helmberger, D. V. (1996). Advancement in source estimation techniques using broadband regional seismograms. Bulletin of the Seismological Society of America, 86(5), 1634-1641.

Zumberge, J. F., Heflin, M. B., Jefferson, D. C., Watkins, M. M., and Webb, F. H. (1997). Precise point positioning for the efficient and robust analysis of GPS data from large networks. Journal of Geophysical Research, 102(B3), 5005-5017.